Effect of Binding of Cd^{2+} on Bacterial Reaction Center Mutants: Proton-Transfer Uses Interdependent Pathways†

Laszlo Gerencser,‡ Antoine Taly,§ Laura Baciou,§ Peter Maroti,‡ and Pierre Sebban*,§

University of Szeged, Szeged, H-6722, Hungary, and Centre de Génétique Moléculaire, Bat. 24, 91198, CNRS, Gif/Yvette, France

Received February 11, 2002; Revised Manuscript Received May 20, 2002

ABSTRACT: In bacterial reaction center of *Rhodobacter sphaeroides*, Cd^{2+} binds in stoichiometric amount to the protein. In the wild type, this results into a notable decrease of the rates of electron-transfer between the two quinone acceptors after the first ($k_{AB}(1)$) and second flash ($k_{AB}(2)$). We have studied these effects in two single mutants, L209PY and L209PF. L209Pro is situated in a protein region rich in hydrogen-bond networks involving water molecules. We show that (1) the combined effects of Cd^{2+} binding and point mutations have a cumulative consequence in the two mutants, decreasing very substantially the observed rates of electron-transfer. Interestingly, the [Cd^{2+}] titration curves of $k_{AB}(2)$ in the L209PY and L209PF mutants are nearly superimposable to those previously reported for the M17DN and L210DN mutants (Paddock, M. L., Feher, G., and Okamura, M. Y. (2000) *Proc. Natl. Acad. Sci U.S.A. 97*, 1548−1553). These observations suggest a common effect of all of these mutations (L209, M17, L210) on the protonation state of the histidine cluster to which Cd^{2+} binds; (2) in the L209PY mutant, the pH titration curves of $k_{AB}(1)$, $k_{AB}(2)$, and k_H^+, the proton-transfer rate at the second flash, are systematically downshifted by 1.5−2 pH units in the presence of 300 μM Cd^{2+}, similarly to the wild type RCs (Gerencser, L., and Maroti, P. (2001) *Biochemistry 40*, 1850−1860). We propose that Cd^{2+} binding influences the electrostatics of interdependent ways of proton penetration within the protein, involving at least, directly or indirectly, L209P, L210D, and M17D, probably in conjunction with hydrogen-bonded connected water molecules.

The light absorption by the bacterial reaction center (RC)[1] protein initiates coupled electron- and proton-transfer reactions leading to the storage of chemical free energy. This protein is considered as a model for studying the dynamic and structural aspects of these molecular events that are central in the membrane bioenergetics of photosynthetic and respiratory systems. After two photochemical steps, which are triggered by the successive absorption of two photons, the protein catalyses the double reduction and double protonation of the final quinone acceptor Q_B to form the dihydroquinone molecule Q_BH_2. The three-dimensional structure of the protein has been determined in the dark (at 2.2 Å resolution) and in the charge-separated state, under continuous light illumination (2.6 Å resolution) (*1*). The primary electron donor is a bacteriochlorophyll dimer (P) situated on the periplasmic side of the complex. The first stable electron acceptor is a quinone molecule, Q_A, situated on the cytoplasmic side of the protein. In *Rhodobacter sphaeroides* RCs, Q_A and Q_B are both ubiquinone 10. At variance to Q_B, Q_A functions as a one-electron acceptor and is never directly protonated. Q_A and Q_B are distant by about 18 Å and are symmetrically situated on opposite sides of a non-heme iron atom.

In native RCs from *R. sphaeroides*, the first electron-transfer process between Q_A^- and Q_B which occurs in 30−400 μs (∼pH 7) (*2*, *3*) is multiphasic. In isolated RCs, the second electron-transfer is biphasic (*4*) and takes place in about 300 μs at pH 7 (*4*, *5*). Both processes have previously been described as being kinetically limited by different molecular mechanisms. Although there is an agreement between the existence of a protein-involved rate-limiting process for the first electron-transfer, the origin of this phenomenon is not yet elucidated. Indeed, the first electron-transfer reaction has been suggested to be limited by a gating process involving the movement of Q_B from a distal (from the iron) position in the neutral form to a proximal position in the light state (*1*, *6*−*8*). However, the recent structural data concerning the L209PY mutant which $k_{AB}(1)$ value is nearly unchanged as compared to the WT, and where Q_B is found in the proximal position in the dark does not support the aforesaid hypothesis (*9*). Alternatively, the protein dynamic motions, which could be coupled to proton rearrangement and water reorientations, have also been proposed to kinetically gate the transfer of the first electron to Q_B (*3*, *10*−*12*).

In isolated RCs, the second electron-transfer process is kinetically coupled to the transfer of the first proton to the

† This work was supported by the Centre National de la Recherche Scientifique and by a BALATON grant (from the Hungarian and by the French Ministère des Affaires Etrangères (No. 00834)).

* To whom correspondence should be addressed. E-mail: sebban@cgm.cnrs-gif.fr. Phone: 33 1 69 82 38 26. Fax: 33 1 69 82 38 32.

‡ University of Szeged.

§ Centre de Génétique Moléculaire.

[1] Abbreviations: L209PY, Pro L209 → Tyr mutant; L209PF, Pro L209 → Phe mutant; LDAO, *N*,*N*′-dimethyldodecylamine *N*-oxide; P, primary electron donor, a noncovalently linked bacteriochlorophyll dimer; Q_A and Q_B, primary and secondary quinones; *R.*, *Rhodobacter*; RC, reaction center; Triton X-100, octylphenol poly(ethylene glycol) ether; UQ_6, ubiquinone-6, 2,3-dimethoxy-5-methyl-6-hexaisoprenyl-1-4-benzoquinone; WT, wild type.

10.1021/bi0256633 CCC: $22.00
Published on Web 06/21/2002

Q_B. A proton-activated electron-transfer mechanism has been proposed which suggests the fast protonation of Q_B, prior to the slower rate-limiting electron-transfer (*6*, *8*, *13*). However, in chromatophores from *R. sphaeroides*, it was shown that, at the first flash, Q_B can be protonated with a p*K* of ~6.8 (*14*), suggesting that there might be no fundamental differences between the first and second electron-transfer processes. In addition, in chromatophores, at pH 7, the same value for the rate of the first ($k_{AB}(1)$) and second electron-transfer ($k_{AB}(2)$) reactions ($k_{AB}(1) \cong k_{AB}(2) \sim 3300\ s^{-1}$) have been measured, suggesting that the same gating process could be involved in both phenomena (*14*).

Recently, it has been discovered that some transition-metal ions (Cd^{2+}, Zn^{2+}, Cu^{2+}, and Ni^{2+}) binds stoichiometrically and reversibly to the RCs in a site, which is different from the iron binding site (*10*, *11*, *15*, *16*). It has initially been suggested that Zn^{2+} could be bound to a cluster of histidine residues beneath the Q_B binding pocket (*10*, *11*, *17*, *18*). Interestingly, the binding of Zn^{2+} was shown to slow the first electron-transfer reaction, probably by altering the localized protein dynamics important for electron-transfer (*10*). Cu^{2+} was also shown to bind in a similar way to the RCs (*11*). Structural data confirmed the localization of the metal binding (Zn^{2+} and Cd^{2+}) to a cluster formed by AspH124, HisH126, and HisH128 and situated on the external cytoplasmic side of the RCs (*15*). Paddock et al. have studied, at pH 8, the consequences of Cd^{2+} binding on the first and second electron-transfer processes in the WT RCs from *R. sphaeroides* (*16*) and in parallel to the AspM17 → Asn and AspL210 → Asn mutants at pH 7.5 (*19*). In the two single mutants, the fixation of Cd^{2+} resulted into a ~70 times reduction of $k_{AB}(2)$, whereas it was ~20 times in the WT. In addition, in the mutants, these authors reported a larger effect on the second electron-transfer as compared to the first one. It was concluded that a unique proton pathway (at least 10^3 more efficient than any other) existed inside the reaction center, which directly involved AspM17, AspL210, and two water molecules, and which entry point consisted of the AspH124, HisH126, and HisH128 cluster. However, very recently, Adelroth et al. (*20*) reported that, in the double mutant where HisH126 and HisH128 have been replaced by alanines, $k_{AB}(1)$ and $k_{AB}(2)$ were only reduced by 10 and 4, respectively. This does not support the fact that this cluster is the unique entry point for protons because a much larger kinetic effect would have been expected in the double mutant.

Very recently, Gerencser and Maroti (*18*) have suggested that the transition-metal effect is essentially due to an electrostatic effect. Indeed, in the WT *R. sphaeroides* RCs, the pH titration curves of the first and second electron-transfers, of the proton-transfer reaction at the second flash, and also of the H^+/Q_A^- and H^+/Q_B^- proton uptake stoichiometries are systematically shifted down by about 2 pH units when a transition metal is added. Because the different protonation channels identified in the RC structure (*1*, *21*) are likely to be under the electrostatic control of the transition-metal fixation, the concepts of a "unique" entry point or pathway for protons seem unlikely (*18*).

In the present work, we have analyzed the electron- and proton-transfer reactions in two single mutants, namely, the ProL209 → Tyr and ProL209 → Phe strains. ProL209 is situated at the border of a sensitive part of the protein, rich in connected hydrogen bonds of water molecules, some of them constituting a continuous water chain from the bulk phase to the Q_B moiety (*21*). We show here that, in a similar way to the WT (*18*), the pH titrations of the electron- and proton-transfer rates measured in the L209PY and L209PF mutants are shifted to lower pH in the presence of Cd^{2+}. Remarkably, the effect of $[Cd^{2+}]$ on the second electron-transfer is very similar as observed for the M17DN and L210DN mutants. This does not support the existence of a highly specific proton pathway within the protein, but rather, the existence of delocalized ways of proton penetration to which L209Pro, M17Asp, L210Asp contribute.

MATERIALS AND METHODS

Bacterial Strains and Growth Conditions. The design of the *R. sphaeroides* wild type or mutant strains harboring *puf*L mutation on pRK404 were previously described (*22*). The cells were grown in Erlenmeyer flasks filled to 50% of the total volume with malate yeast medium supplemented with kanamycin (20 μg/mL) and tetracycline (2 μg/mL). The cultures were grown in darkness at 30 °C on a gyratory shaker (100 rpm).

Biochemical Techniques. R. sphaeroides strains harboring native or mutations at L209 were disrupted by sonication in 20 mM Tris (pH 8) buffer in the presence of DNAse and PMSF (1 mM). The intracytoplasmic membranes were purified as described in (*22*). The membrane solubilization was done first by addition of LDAO (Fluka Chemie) to a final concentration of 0.35% in the presence of 100 mM NaCl. The RCs were extracted by a second addition of LDAO to a final concentration of 0.8% in similar conditions. The solubilized RCs were subsequently purified on a DEAE Sepharose CL-6B (Pharmacia) column and eluted at an ionic strength equivalent to 250 mM NaCl. The ratio of absorbance at 280/802 nm was in the range 1.5−1.8 for all RC preparations.

The RC isolation and purification were achieved according to the procedure described in ref *22*.

Flash-Induced Absorbance Changes. The homemade flash (YAG laser at 532 nm) induced absorbance change apparatus has previously been described (*23*).

Charge recombination kinetics. The rate constant values of the $P^+Q_B^- \rightarrow PQ_B$ (k_{BP}) charge recombinations were measured at 430 nm.

Electron-Transfer Kinetics. The kinetics of the first electron-transfer from Q_A^- to Q_B were measured at 750 nm, in the electrochromic band shift of the bacteriopheophytins. These experiments were done in the presence of 25 μM UQ_6 (coenzyme Q_6; Sigma) and ~2 μM RC.

The kinetics of transfer of the second electron from Q_A^- to Q_B^- were measured at 450 nm in the presence of reduced cytochrome *c* (20 μM), 25 μM UQ_6, and ~ 2 μM RC.

Proton-Transfer Kinetics. The RCs were extensively dialyzed against 50 mM NaCl and 0.03% Triton X-100 (Sigma) during 36 h at 4 °C. Under these conditions, the Tris buffer concentration was kept below 10 μM and the LDAO micelles were exchanged to Triton X-100 micelles. The proton uptake kinetics by the RCs were measured on a homemade spectrophotometer (*23*) by following the absorption changes at 585 nm (isosbestic point of P/P^+ absorption changes) of pH sensitive dyes after one saturating (Yag) laser

Table 1: Rate Constant Values for the $P^+Q_B^-$ Charge Recombination for the Native, the L209PY, and the L209PF RC Mutants in the Absence and Presence of 1 mM Cd^{2+} at pH 8.5, 7.8, and 6.8[a]

	k_{BP} (0) (s^{-1})	k_{BP} (Cd^{2+}) (s^{-1})
	L209PY	
pH 8.5	0.62	0.48
pH 7.8	0.60	0.48
pH 6.8	0.56	0.40
	L209PF	
pH 8.5	0.68	0.41
pH 7.8	0.67	0.40
pH 6.8	0.50	0.35
	WT	
pH 8.5	1.15[b]	1.15[b]
pH 7.8	1.05[b]	1.05[b]
pH 6.8	0.80[b]	0.80[b]

[a] The standard deviation of the results is 10%. [b] Data from ref *18*.

Table 2: Parameters Related to the First Electron-Transfer for the Native, the L209PY, and the L209PF RC Mutants in the Absence and Presence of Cd^{2+} (1 mM), pH 8

	k_{AB}(1) (0) (s^{-1})	k_{AB}(1) (Cd^{2+}) (s^{-1})	k_{AB}(1) (0)/ k_{AB}(1) (Cd^{2+})
L209PY	9100	120	75
L209PF	150	120	1.25
WT	9600	900	11

flash at 532 nm. The final proton uptake signal was obtained by subtracting the signal of the buffered sample (10 mM) from that of the unbuffered sample. The proton uptake by the RCs (~2 μM) was measured at room temperature in the presence of 20 μM *o*-cresol red or cresol-phthaleine, depending on the pH range.

RESULTS

Charge Recombination Processes. The k_{BP} values determined at pH 8.5, 7.8, and 6.8 in the absence and in the presence of 1 mM Cd^{2+} for the L209PY and L209PF mutant RCs and for the WT are presented in Table 1. Similarly to what previously reported for the WT *R. sphaeroides*, the k_{BP} values measured at these pH are not notably affected by the presence of 1 mM Cd^{2+} (*18*, *19*). In the L209PY and L209PF mutants, at pH 7.8, k_{BP} is slightly decreased by the presence of Cd^{2+} (0.48 and 0.40 s^{-1}, respectively) as compared to the values measured in the absence of Cd^{2+} (0.60 and 0.67 s^{-1}, respectively). The same trend is detected at pH 6.8 and pH 8.5.

Effect of Cd^{2+} Concentration on the First Electron-Transfer Reaction. At pH 7.8, in the WT, upon saturating addition of Cd^{2+} (>10 μM), k_{AB}(1) is decreased about 10 times from 9600 to 900 s^{-1} (Table 2). The magnitude of the Cd^{2+} effect agrees with previous reports (*18*, *19*).

In the case of the two mutants, the situation is quite different. At pH 7.8, in the L209PY mutant, k_{AB} (1) (~9100 s^{-1}) measured in the absence of Cd^{2+} is not much changed as compared to the native RCs. However, a large effect on k_{AB}(1) is observed upon Cd^{2+} addition. Although a small part of the overall kinetics remains fast (~9100 s^{-1}), upon addition of Cd^{2+} the main part of the kinetics is much slowed. This slow phase corresponds to a rate reduced by about 30 times (~350 s^{-1}), even upon very small additions of Cd^{2+} (~0.6 μM). The Cd^{2+} titration curve of the slow phase of k_{AB}(1) is presented in Figure 1. Interestingly, a plateau is observed up to a Cd^{2+} concentration of about 70 μM above which k_{AB}(1) titrates down to about 120 s^{-1} at $[Cd^{2+}] = 1$ mM. Therefore, upon $[Cd^{2+}] = 1$ mM, the first electron-transfer is reduced by a factor of ~75 in the L209PY mutant. Although not very pronounced, the titration of k_{AB}(1) from ~350 s^{-1} down to ~120 s^{-1} may reflect the presence of a weaker binding site for Cd^{2+}. A quantitative analysis assuming a two-sites titration would be required to account for this behavior. However, considering the weak effect detected in the L209PY mutant and its absence in the L209PF mutant, we decided not to go to such a treatment.

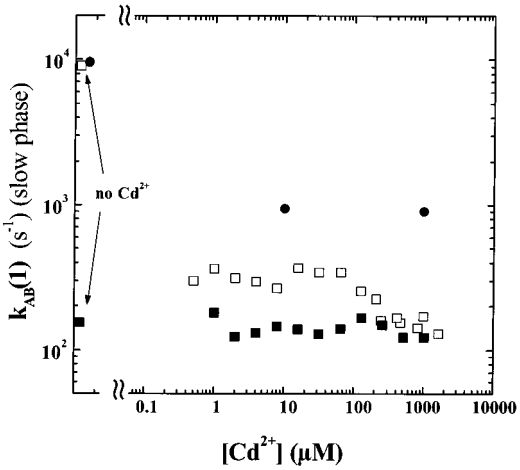

FIGURE 1: Effect of Cd^{2+} concentration on the slow phase of k_{AB}(1) (detected at 750 nm) in the RCs (~2 μM) from the L209PY (□) and L209PF (■) mutants and from the WT (●) *R. sphaeroides*. Conditions: 10 mM Tris (pH 7.8), 100 mM NaCl, 0.05% LDAO, and 25 μM UQ_6.

The situation is different for the L209PF mutant RCs. In the absence of Cd^{2+}, k_{AB}(1) is already substantially reduced as compared to the native RCs. At pH 7.8, k_{AB}(1) ~ 150 s^{-1}. Interestingly, the addition of Cd^{2+} up to 1 mM does not notably further reduce k_{AB}(1) (Figure 1 and Table 2). Indeed, the value observed at any Cd^{2+} concentration, ~120 s^{-1}, is nearly the same as for the L209PY mutant at 1 mM Cd^{2+}.

Effect of [Cd^{2+}] on the Second Electron-Transfer Reaction in the L209Y and L209F Mutants. In the native RCs, k_{AB}(2) is about 1000 s^{-1} at pH 7.8. As previously reported, upon addition of Cd^{2+}, a slow phase appears whose amplitude titrates with a dissociation constant of K_d ~ 0.3 μM (see Table 3) (*16*). We have measured k_{AB} (2) in the presence of 10 μM and 1 mM Cd^{2+}. The same values of ~50 s^{-1} were found in both cases (Figure 2 and Table 3). This is in good agreement with the value of ~60 s^{-1} reported for the WT at pH 7.7, for Cd^{2+} concentrations above ~10 μM (*16*, *18*).

The [Cd^{2+}] titrations of the slow phase of k_{AB}(2) in the L209PY and L209PF mutants, measured at pH 7.8, are presented in Figure 2. In the L209PY mutant RCs, the slow phase of k_{AB}(2) titrates from ~55 s^{-1} in the presence of <0.5 μM Cd^{2+} to about 7 s^{-1} in the presence of 1 mM Cd^{2+}. The Cd^{2+} titration curve for the slow phase of k_{AB}(2) in the L209PF mutant is superimposable within the error of the experiment to that of the L209PY mutant. Indeed, in the L209PF mutant, the rate of the slow phase of k_{AB}(2) is ~55 s^{-1} in the presence of very small amounts of Cd^{2+} and titrates to about 5 s^{-1} in the presence of 1 mM Cd^{2+}. In the L209PF

Table 3: Parameters Related to the Second Electron-Transfer and Cd^{2+} Binding for the Native, the L209PY, and the L209PF RC Mutants in the Absence and Presence of Cd^{2+} (1 mM), pH 7.8

	$k_{AB}(2)$ (0) (s^{-1})	$k_{AB}(2)$ (Cd^{2+}) (s^{-1})	$k_{AB}(2)$ (0)/ $k_{AB}(2)$ (Cd^{2+})	k_{off} (2) (s^{-1})	k_{on} ($\mu M^{-1}\cdot s^{-1}$)	K_d (μM)
L209PY	370	6.5	57	45	30	1.5
L209PF	50	4	13	50	2	25
WT	1000	50	20			~0.3[a]

[a] Data from Paddock et al. (*32*), pH 7.7.

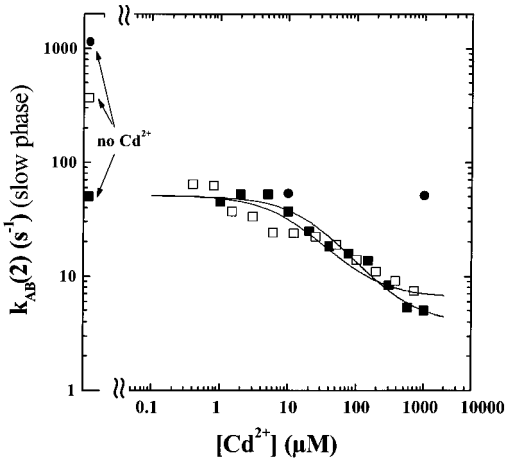

FIGURE 2: Effect of Cd^{2+} concentration on the slow phase of $k_{AB}(2)$ (detected at 450 nm) in the RCs (~2 μM) from the L209PY (□) and L209PF (■) mutants and from the WT (●) *R. sphaeroides*. Conditions: 10 mM Tris (pH 7.8), 100 mM NaCl, 0.05% LDAO, 25 μM UQ_6, and 20 μM reduced cytochrome *c*.

Scheme 1: Hypothesis Proposed in Ref *19* to Account for Cd^{2+} Binding to Reaction Centers[a]

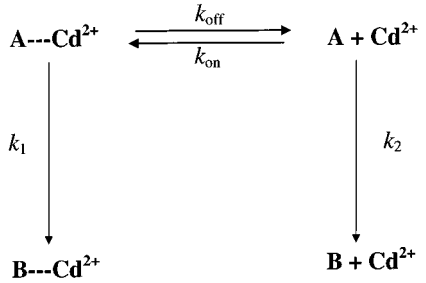

[a] A = ($Q_A^-Q_B^-$) and B = ($Q_AQ_BH^-$). A---Cd^{2+} and B---Cd^{2+} represent the A and B states with Cd^{2+} bound to the RC. A + Cd^{2+} and B + Cd^{2+} represent the A and B states with unbound Cd^{2+}. $k_1 = k_{AB}(2)$ (Cd^{2+}) and $k_2 = k_{AB}(2)$ (0). Solution of the differential equations describing the decay of A---Cd^{2+} and A + Cd^{2+} leads to the time dependence of [A---Cd^{2+}] (*t*) (*19*): [A---Cd^{2+}] (*t*) = $[0.5(a - b + c)/a]\exp[-0.5(b + c - a)t] + [0.5(a + b - c)/a]\exp[-0.5(b + c + a)t]$, where $a = \{k_1^2 + 2k_1k_{off} - 2k_1k_2 - 2k_1k_{on}[Cd^{2+}] + k_{off}^2 - 2k_{off}k_2 + 2k_{on}[Cd^{2+}]k_{off} + k_2^2 + 2k_{on}[Cd^{2+}]k_2 + (k_{on}[Cd^{2+}])^2\}^{1/2}$, $b = k_1 + k_{off}$, and $c = k_2 + k_{on}[Cd^{2+}]$. The [$Cd^{2+}$] titration curves for the L209PY and L209PF RC mutants presented in Figure 2 were fitted by the above equation.

mutant, the rate of the slow phase of $k_{AB}(2)$ at low Cd^{2+} concentrations is not much affected by the presence of Cd^{2+}, as observed above for $k_{AB}(1)$.

Fitting Procedure of the Second Electron-Transfer Rates versus [Cd^{2+}]. To fit the curves of Figure 2, we have used the simple model presented in Scheme 1, taken from ref *19*. These authors have assumed that the reaction center protein has two different $k_{AB}(2)$ rates depending on Cd^{2+} being bound or not to the RC ($k_{AB}(2)$ (Cd^{2+}) and $k_{AB}(2)$ (0), respectively). The equilibrium between the bound Cd^{2+} and unbound Cd^{2+} states is governed by the relative values of k_{on} (second-order rate for Cd^{2+} binding) and k_{off} (first-order unbinding rate for Cd^{2+}). The time resolution of this system is described by the equation derived in ref *19* and presented here in the caption of Scheme 1.

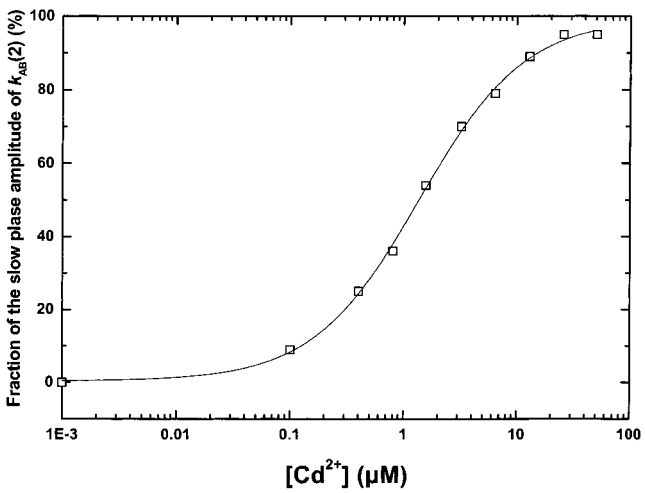

FIGURE 3: Cd^{2+} titration of the fraction of the slow phase amplitude of $k_{AB}(2)$ (measured at 450 nm) in the L209PY RCs. Conditions: 10 mM Tris (pH 7.8), 100 mM NaCl, 0.05% LDAO, 25 μM UQ_6, and 20 μM reduced cytochrome *c*.

The electron-transfer kinetics and Cd^{2+} binding parameters deduced from the fitting of the $k_{AB}(2)$ data for the L209PY and L209PF mutants are presented in Table 3. The fitting of the slow phase of $k_{AB}(2)$ leads to values for $k_{AB}(2)$ (Cd^{2+}) of ~6.5 and 4 s^{-1}, respectively for the L209PY and L209PF mutants. These are ~57-fold and ~13-fold decreases, respectively, of the second electron-transfer rate. Interestingly, in the case of the L209PY mutant, the $k_{AB}(2)$ (Cd^{2+}) values and the extent of decrease of $k_{AB}(2)$ are very similar to what was previously reported for the DN(M17) and DN(L210) mutant RCs from *R. sphaeroides* (*19*).

The Cd^{2+} binding parameters related to the second electron-transfer process for the L209PY mutant is presented in Table 3. The K_d values derived from the fit of the $k_{AB}(2)$ curves are about 1.5 and 25 μM for the L209PY and L209PF mutants, respectively. In the L209PY RC, we have measured this value directly by titrating the apparition of the slow phase of $k_{AB}(2)$. These data are displayed in Figure 3. This independent measurement is consistent with a K_d value of 1.35 ± 0.3 μM in good agreement with the value deduced from the fit of Figure 2. This validates the model proposed in ref *19*.

pH Titration of the $k_{AB}(1)$ Values in the L209PY Mutant. The pH titration curves of $k_{AB}(1)$ in the L209PY mutant in the absence and in the presence of 300 μM Cd^{2+} are presented in Figure 4. In the presence of Cd^{2+}, we fitted the data with a biexponential model. Even at high Cd^{2+}

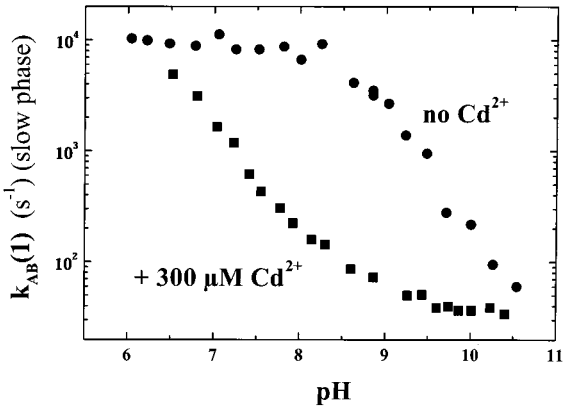

FIGURE 4: pH titration of $k_{AB}(1)$ (measured at 750 nm) in the RCs from the L209PY mutant in the absence (●) or in the presence (■) of 300 μM Cd^{2+}. Conditions: 10 mM Tris (pH 7.8), 100 mM NaCl, 0.05% LDAO, and 25 μM UQ_6.

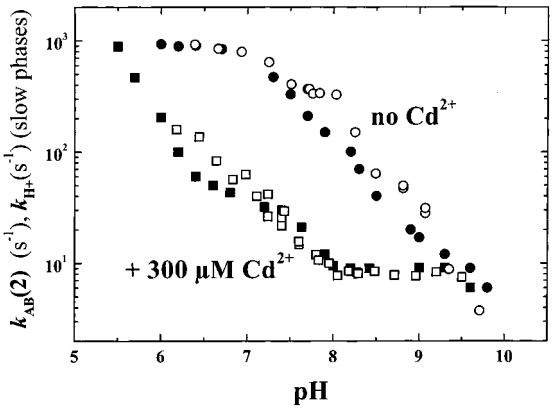

FIGURE 5: pH titration of $k_{AB}(2)$ (○, □) (measured at 450 nm) and of k_H^+ (●, ■) (measured at 585 nm in the presence of dyes (see Material and Methods)) in the RCs from the L209PY mutant in the absence (or in the presence of 300 μM Cd^{2+}). Conditions: 10 mM Tris (pH 7.8), 100 mM NaCl, 0.05% TX-100, 25 μM UQ_6, and 25 μM reduced cytochrome *c*.

concentration, some fast phase (same value as in the absence of Cd^{2+}) still remained (~20−30%). Therefore, in the presence of Cd^{2+}, $k_{AB}(1)$ represents the slow (major) part of the decay. In the absence of Cd^{2+}, a plateau is observed up to pH ~ 8.5 with a rate of about 10^4 s^{-1}. Above this pH value, $k_{AB}(1)$ varies with a slope proportional to ~$[H]^1$. In the presence of 300 μM Cd^{2+}, the data points for $k_{AB}(1)$ are shifted to lower pH values by about 2 pH units. Interestingly, below pH 6.5−7 and above pH 10.5, both data (+ or − Cd^{2+}) reach nearly the same values (~10^4 and ~20, respectively). Therefore, the range for $k_{AB}(1)$ values is not affected by the presence of 300 μM Cd^{2+} but only shifted toward lower pH.

pH Titrations of the Rates of Electron and Proton-Transfer at the Second Flash in the L209PY Mutant. The pH titration curves of $k_{AB}(2)$ and k_H^+, the rate of proton-transfer at the second flash, in the L209PY mutant in the absence and presence of 300 μM Cd^{2+} are presented in Figure 5. It has previously been demonstrated that K_d for Cd^{2+} binding depends on pH and notably increases at low pH. We used a biexponential function to fit our data at all pH values and took only the slow component as the value of $1/k_{AB}(2)$.

We have previously published the pH titration of $k_{AB}(2)$ in the absence of Cd^{2+} (*22*, *24*). The k_H^+ titration curve, measured here, follows, within the experimental error, the $k_{AB}(2)$ curve. Indeed, at pH 6 k_H^+ is about 1000 s^{-1}. Above pH ~7.2, the rate drops with a slope nearly proportional to $[H^+]$ and leading to $k_H^+ \sim 4$ s^{-1} at pH 10.

In the presence of 300 μM Cd^{2+}, the superimposition of the $k_{AB}(2)$ and k_H^+ remains, at least down to pH 6. Similarly as observed for the first electron-transfer process, the presence of Cd^{2+} shifts by about 2 pH units the rate titration curves measured in the absence of metal. At pH 5.5, the k_H^+ values measured in the presence of Cd^{2+} match (~1000 s^{-1}) those determined in the absence of metal. The slopes of the $k_{AB}(2)$ and k_H^+ curves in the presence of metal are close to a proportionality of $[H^+]^1$. Above pH 8, the $k_{AB}(2)$ and k_H^+ titration curves reach values of ~8 s^{-1}, very similar to that measured in the absence of metal but at pH 9.6.

DISCUSSION

Recent structural (*15*) and spectroscopic (*10*, *11*, *16*, *18*) data achieved on WT RCs from *R. sphaeroides* have demonstrated that transition-metal ions, like Cd^{2+}, bind to the surface of the protein and decrease the electron- and proton-transfer rates at the first and second flashes, respectively. It has been proposed that, on one hand, the decrease of these rates is due to the electrostatic influence of the charge carried by the Cd^{2+} ion and, on the other hand, that the apparent dissociation constant for Cd^{2+} binding is governed or at least strongly influenced by the protonation state of the HisH128 and HisH126 cluster (*18*).

To further investigate these effects and to probe the penetration pathways of protons within the protein, we have measured the effect of Cd^{2+} binding on the electron- and proton-transfer kinetics in RC mutants in which L209Pro was changed to Tyr and Phe. We have recently reported the stoichiometries of proton uptake by the PQ_A^- and PQ_B^- states in the L209PY and L209PF mutants (*25*). We have shown that the replacement of L209Pro by aromatic residues is likely to affect the functioning of protonation groups lying between Q_B and the water phase and which role is to provide protons to the close environment of Q_B (i.e., to the ultimate proton donors to Q_B (L212Glu and L213Asp)). The present data support such a figure in which Cd^{2+} fixation influences the electrostatic properties of these groups (including hydrogen-bond networks of connected waters) but not necessarily of the very close environment of Q_B.

Effect of the Mutations on K_d for Cd^{2+} Binding. One of the main observations is that, at pH 7.8, the titration curves of the slow phase of $k_{AB}(2)$ versus $[Cd^{2+}]$ display similar extended shapes and close values in the L209PY and L209PF mutants as those previously measured in the M17Asp → Asn and L210Asp → Asn mutants (*19*). Taking the same model as these authors (*19*), notably higher values of K_d for Cd^{2+} binding were derived in the L209Pro → Tyr mutant (1.5 μM), the L209Pro → Phe (25 μM), than in the WT at pH 7.8 (~0.3 μM) (*18*, *19*). In the M17Asp → Asn and L210Asp → Asn mutants, K_d was determined to be 3.1 and 1.2 μM, respectively (*19*). Therefore, all four mutations lead to a notable increase of K_d. A careful examination of the three-dimensional structure of the RCs of the two L209 mutants does not suggest any important rearrangements of HisH126, HisH128, or AspH124. We therefore do not favor a structural change in the L209 mutants at the level of binding site for Cd^{2+} that could explain for the observed increased K_d values.

Measuring the pH dependence of K_d for Cd^{2+}, Gerencser and Maroti (*18*) have recently suggested that, in the WT, K_d is mainly determined by the protonation state of HisH126 and HisH128. In support of this hypothesis, we have calculated the protonation states of HisH128 and HisH126 in the L209F mutant (Taly, A., Sebban, P., Baciou, L., Smith, J. C., and Ullmann, M. Unpublished data). At neutral pH, both histidine appear to be more protonated than in the WT, therefore leading to an increase of K_d. Very recently, Sagle et al. (*26*) have proposed that Cd^{2+} and protons compete for the binding on the histidines. The hypothesis that the K_d for transition-metal ions binding, is crucially dependent on the protonation states of its ligand residues has recently been proposed for the binding of Zn^{2+} in the distal finger motif of the HIV-1 nucleocapsid protein (*27*). Indeed, it has been shown that each protonation step of the coordination complex (3 Cys and 1 His) decreases the Zn^{2+} -binding constant by 4 orders of magnitude.

We propose that, in the L209, M17, and L210 mutants, the increase of K_d is mainly due to the pK_a increase of the histidines to which Cd^{2+} is bound. The L209 mutations take place in a region of the protein rich in water molecules involved in hydrogen-bond networks. This is also the case for the M17 and L210 positions. We suggest that the systematic increase of the K_d values determined in all four mutants (L209PY, L209PF, L210DN, M17DN) may result from a similar modification of the structure of the water hydrogen-bond network present in this region of the protein. This can, in turn, affect the local dielectric property of the protein and modify the protonation states of HisH126 and HisH128. It is also possible that residues important for their (distant) electrostatic influence on HisH126 and HisH128 have been modified in a similar way in all of the mutants. We have reported in the two L209 aromatic mutants some displacements of AspL213 and GluH173 (*9*). These residues may have also been modified in the M17DN and L210DN mutants, resulting in similar effects on the pK_a of HisH126 and HisH128.

Effects of Cd^{2+} on the First Electron-Transfer. The $k_{AB}(1)$ value measured in the L209PY mutant (9100 s^{-1}) in the absence of Cd^{2+} is close to that of the WT (~9600 s^{-1}). However, at pH 7.8, in the presence of 1 mM Cd^{2+} concentration, $k_{AB}(1)$ is much more reduced in the L209PY mutant (~120 s^{-1}; ~75 times) than in the WT (~700 s^{-1}; ~10 times). $k_{AB}(1)$ is mainly governed by the protonation state of L212Glu (*17*, *28*−*30*). We have previously suggested that the L209PY mutantion may have disorganized the hydrogen-bond network involving water molecules and protonatable groups, which may serve as proton provision for L212Glu (*24*). Indeed, we have shown that the protonation state of the cluster containing L212Glu is unaffected by the mutation. Therefore, providing protons to L212Glu may be slowed in the mutant. The large effect of Cd^{2+} in the L209PY mutant may therefore result from a further energetic disorganization of the proton providing groups to GluL212 due to the shift of their pK_a.

Interestingly, in the L209F mutant, $k_{AB}(1)$ is already very decreased (~150 s^{-1}), even in the absence of Cd^{2+}. Similarly to the L209Y mutant, we have interpreted this as due to a strong disorganization of the proton providing groups (and not to L212Glu itself) (*24*). As displayed in Figure 1, Cd^{2+} up to 1 mM does not further reduce $k_{AB}(1)$. In addition, at high Cd^{2+} concentrations, $k_{AB}(1)$ values are the same for the two L209 mutants. It seems therefore that the $k_{AB}(1)$ value (100−150 s^{-1}) reached at high Cd^{2+} concentrations is the lowest that can be reached when the combined effects of the aromatic mutation and Cd^{2+} fixation are added. This rate may correspond to the slow proton delivery rate to L212Glu, which becomes the rate-limiting factor for the first electron-transfer process under Cd^{2+} fixation.

Effects of Cd^{2+} on the Second Electron-Transfer. It is noteworthy that the Cd^{2+} titrations of the slow phase of $k_{AB}(2)$ are very similar for the L209 mutants and for the previously reported M17Asp → Asn and L210Asp → Asn mutants (*19*). In particular, $k_{AB}(2)$ values at low Cd^{2+} concentrations but also the magnitude of the decrease of $k_{AB}(2)$ in the [Cd^{2+}] range from 1 μM to 1 mM are very close; this reduction is ~12 for the L209PF mutant and ~10 for the L209PY mutant, 10 for the L210DN mutant, and ~12 for the M17DN mutant.

It has previously been shown that, in the presence of Cd^{2+}, the proton coupled-second electron-transfer reaction becomes proton-limited (*16*, *19*). Therefore, the aforesaid similar reductions of $k_{AB}(2)$ in the mutants suggest a common rate limitation for proton-transfer upon fixation of Cd^{2+}. Taking into account the same pH shift of the $k_{AB}(2)$ and k_H^+ curves (Figure 4) and the low sensitivity of k_{BP} to Cd^{2+} binding in the L209 mutants, we suggest that Cd^{2+} fixation shifts the pK_a of groups which are providing protons to L213Asp. Indeed, L213Asp has been shown to be directly involved in the ultimate donation of first proton to Q_B^- at the second flash (*31*). Therefore, reducing the transfer rate for the first proton from the proton providing reservoir to L213Asp would result in the overall slowing down of the second flash electron-transfer kinetics.

At variance to the very notable increase of the K_d value for Cd^{2+} binding in the L209 mutants as compared to the WT, the pH titration curves of $k_{AB}(1)$ (Figure 4), $k_{AB}(2)$ (Figure 5), and k_H^+ (Figure 5) measured in the L209PY systematically display nearly the same downshift of about 1.6−2.0 pH units as observed in the WT (*18*). We may therefore consider that, in the L209PY mutant and the WT, the electrostatic effect induced by the Cd^{2+} binding at the level of the groups whose pK_a values govern the pH titration curves of the electron- and proton-transfer rates is nearly the same. Conversely, we observe that the L209Pro → Tyr mutation affects K_d (i.e., probably the protonation states of HisH126 and HisH128). This may suggest that these two crossed effects are not correlated and that the effect of Cd^{2+} binding is very delocalized at the level of several different groups providing protons (perhaps cooperatively) in the WT to the ultimate proton acceptor−donor residues close to Q_B.

CONCLUSION

It is remarkable that the four reaction center mutants studied here (L209PY and L209PF) and previously (L210DN and M17DN) display a notable decrease of Cd^{2+} binding affinity (due to increases of k_{off}) and very similar reductions of $k_{AB}(2)$ upon high Cd^{2+} concentration. A common structural and subtle rearrangement of the charge distribution, propagating its effect to the surface histidine cluster, is probable. This can be due to the modifications induced by the four mutations on the hydrogen-bond networks and perhaps on

important residues for the overall electrostatics of this region, like AspL213 and GluH173.

REFERENCES

1. Stowell, M. H., McPhillips, T. M., Rees, D. C., Soltis, S. M., Abresch, E., and Feher, G. (1997) *Science 276*, 812−816.
2. Li, J., Gilroy, D., Tiede, D. M., and Gunner, M. R. (1998) *Biochemistry 37*, 2818−2829.
3. Tiede, D. M., Vazquez, J., Cordova, J., and Marone, P. A. (1996) *Biochemistry 35*, 10763−10775.
4. Takahashi, E., and Wraight, C. A. (1992) *Biochemistry 31*, 855−866.
5. Paddock, M. L., Rongey, S. H., McPherson, P. H., Juth, A., Feher, G., and Okamura, M. Y. (1994) *Biochemistry 33*, 734−745.
6. Okamura, M. Y., Paddock, M. L., Graige, M. S., and Feher, G. (2000) *Biochim. Biophys. Acta 1458*, 148−163.
7. Graige, M. S., Feher, G., and Okamura, M. Y. (1998) *Proc. Natl. Acad. Sci U.S.A. 95*, 11679−11684.
8. Graige, M. S., Paddock, M. L., Feher, G., and Okamura, M. Y. (1999) *Biochemistry 38*, 11465−11473.
9. Kuglstatter, A., Ermler, U., Michel, H., Baciou, L., and Fritzsch, G. (2001) *Biochemistry 40*, 4253−4260.
10. Utschig, L. M., Ohigashi, Y., Thurnauer, M. C., and Tiede, D. M. (1998) *Biochemistry 37*, 8278−8281.
11. Utschig, L. M., Poluektov, O., Tiede, D. M., and Thurnauer, M. C. (2000) *Biochemistry 39*, 2961−2969.
12. Maroti, P., and Wraight, C. A. (1997) *Biophys. J. 73*, 367−381.
13. Graige, M. S., Paddock, M. L., Bruce, J. M., Feher, G., and Okamura, M. Y. (1996) *J. Am. Chem. Soc. 118*, 9005−9016.
14. Lavergne, J., Matthews, C., and Ginet, N. (1999) *Biochemistry 38*, 4542−4552.
15. Axelrod, H. L., Abresch, E. C., Paddock, M. L., Okamura, M. Y., and Feher, G. (2000) *Proc. Natl. Acad. Sci. U.S.A. 97*, 1542−1547.
16. Paddock, M. L., Graige, M. S., Feher, G., and Okamura, M. Y. (1999) *Proc. Natl. Acad. Sci. U.S.A. 96*, 6183−6188.
17. Adelroth, P., Paddock, M., Sagle, L. B., Feher, G., and Okamura, M. Y. (2000) *Proc. Natl. Acad. Sci. U.S.A. 97*, 13096−13091.
18. Gerencser, L., and Maroti, P. (2001) *Biochemistry 40*, 1850−1860.
19. Paddock, M. L., Feher, G., and Okamura, M. Y. (2000) *Proc. Natl. Acad. Sci. U.S.A. 97*, 1548−1553.
20. Adelroth, P., Paddock, M. L., Tehrami, A., Beatty, J. T., Feher, G., and Okamura, M. Y. (2001) *Biochemistry 40*, 14538−14546.
21. Ermler, U., Fritzsch, G., Buchanan, S. K., and Michel, H. (1994) *Structure 2*, 925−936.
22. Baciou, L., and Michel, H. (1995) *Biochemistry 34*, 7967−7972.
23. Miksovska, J., Kálmán, L., Schiffer, M., Maróti, P., Sebban, P., and Hanson, D. K. (1997) *Biochemistry 36*, 12216−12226.
24. Tandori, J., Sebban, P., Michel, H., and Baciou, L. (1999) *Biochemistry 40*, 13179−13187.
25. Tandori, J., Alexov, E., Maroti, P., Sebban, P., and Baciou, L. (2002) *Proc. Natl. Acad. Sci., U.S.A. 99*, 6702−6706.
26. Sagle, L., Paddock, M. L., Feher, G., and Okamura, M. Y. (2002) *Biophys. J. 957.*
27. Bombarda, E., Morellet, N., Cherradi, H., Spiess, B., Bouaziz, S., Grell, E., Roques, B. P., and Mély, Y. (2001) *J. Mol. Biol. 310*, 659−672.
28. Hienerwadel, R., Grzybek, S., Fogel, C., Kreutz, W., Okamura, M. Y., Paddock, M. L., Breton, J., Nabedryk, E., and Mantele, W. (1995) *Biochemistry 34*, 2832−2843.
29. Nabedryk, E., Breton, J., Hienerwadel, R., Fogel, C., Mäntele, W., Paddock, M. L., and Okamura, M. Y. (1995) *Biochemistry 34*, 14722−14732.
30. Mezzetti, A., Nabedryk, E., Breton, J., Okamura, M. Y., Paddock, M. L., Giacometti, G., and Leibl, W. (2002) *Biochim. Biophys. Acta*, in press.
31. Takahashi, E., and Wraight, C. A. (1990) *Biochim. Biophys. Acta 31*, 855−866.
32. Paddock, M. L., Adelroth, P., Chang, C., Abresch, E. C., Feher, G., and Okamura, M. Y. (2001) *Biochemistry 40*, 6893−6902.

BI0256633